JCB Article

Iqg1p links spatial and secretion landmarks to polarity and cytokinesis

Mahasin A. Osman,[1] James B. Konopka,[2] and Richard A. Cerione[1]

[1]Department of Molecular Medicine, College of Veterinary Medicine, Cornell University, Ithaca, NY 14853
[2]Department of Molecular Genetics and Microbiology, State University of New York, Stony Brook, NY 11794

Cytokinesis requires the polarization of the actin cytoskeleton, the secretion machinery, and the correct positioning of the division axis. Budding yeast cells commit to their cytokinesis plane by choosing a bud site and polarizing their growth. Iqg1p (Cyk1p) was previously implicated in cytokinesis (Epp and Chant, 1997; Lippincott and Li, 1998; Osman and Cerione, 1998), as well as in the establishment of polarity and protein trafficking (Osman and Cerione, 1998). To better understand how Iqg1p influences these processes, we performed a two-hybrid screen and identified the spatial landmark Bud4p as a binding partner. Iqg1p can be coimmunoprecipitated with Bud4p, and Bud4p requires Iqg1p for its proper localization. Iqg1p also appears to specify axial bud-site selection and mediates the proper localization of the septin, Cdc12p, as well as binds and helps localize the secretion landmark, Sec3p. The double mutants *iqg1Δsec3Δ* and *bud4Δsec3Δ* display defects in polarity, budding pattern and cytokinesis, and electron microscopic studies reveal that these cells have aberrant septal deposition. Taken together, these findings suggest that Iqg1p recruits landmark proteins to form a targeting patch that coordinates axial budding with cytokinesis.

Introduction

A critical step in eukaryotic cell division involves the correct positioning of the division plane, which in turn determines the segregation of one intact genome into each cell progeny. Eukaryotic organisms utilize diverse mechanisms to define their division planes. The budding yeast, *Saccharomyces cerevisiae*, uses cortical cues to mark the division site by initiating a bud early in G1, thereby committing to its division axis (Chant, 1996). Haploid yeast divide in such a manner that a bud is formed next to the previous division site, thus resulting in an axial budding pattern (Chant and Herskowitz, 1991). It is believed that a septin ring marks the division site at G1 and persists to assemble other axial markers as well as proteins involved in cytokinesis (for review see Chant, 1996, 1999). Genetic analyses have identified Bud3p, Bud4p, Axl1, and the transmembrane protein Bud10p as axial markers involved in bud-site selection (for reviews see Sanders and Fields, 1995; Chant, 1996, 1999; Madden and Snyder, 1998). The molecular mechanism by which the septin ring localizes to the bud site to position these bud site selection markers (future division-site) is poorly understood.

Address correspondence to Mahasin A. Osman, Department of Molecular Medicine, College of Veterinary Medicine, Cornell University, Ithaca, NY 14853-6401. Tel.: (607) 253-3883. Fax: (607) 253-3659. E-mail: mo28@cornell.edu

*Abbreviation used in this paper: IBID, Iqg1-Bud4 interacting domain.

Key words: Iqg1; Bud4; Sec3; polarity; cytokinesis

Once a bud site is selected, polarized secretion is directed to that site (Lew and Reed, 1995). Fusion of the secretory vesicles at the target site requires a protein complex, the exocyst (Finger et al., 1998), composed of the Sec3, -5, -6, -8, -10, and -15 proteins. Some of the exocyst members, such as Sec3p and Sec4p, localize to the bud tip (Bowser et al., 1992; TerBush and Novick, 1995). After nuclear division, the exocyst reorients to the mother bud neck to promote cytokinesis (Finger et al., 1998). Thus, budding and cytokinesis both involve directed secretion. Furthermore, some *sec3* mutants exhibit a random budding pattern, suggesting the involvement of the complex in bud-site selection (Finger et al., 1998). Nevertheless, no direct molecular link between the exocyst and the bud site selection proteins has yet been reported.

Sec3p localizes to growth sites independent of the other exocyst components, actin, or septins, indicating that Sec3p works as a landmark for secretion (Finger et al., 1998). The polarized localization of Sec3p has been suggested to require the kinase Cdc28p (Finger et al., 1998), as well as the small GTPases Rho1 (Guo et al., 2001) and Cdc42p (Zhang et al., 2001). It is also believed that the positional signal imposed by the septin and bud site selection proteins is interpreted by Cdc42p and other polarity establishment proteins to polarize the actin cytoskeleton (Johnson and Pringle, 1990) and the secretory pathway (Finger et al., 1998). The Cdc42 effector(s) that mediates these functions and the mechanism by which it is achieved remain important questions. However, one intriguing

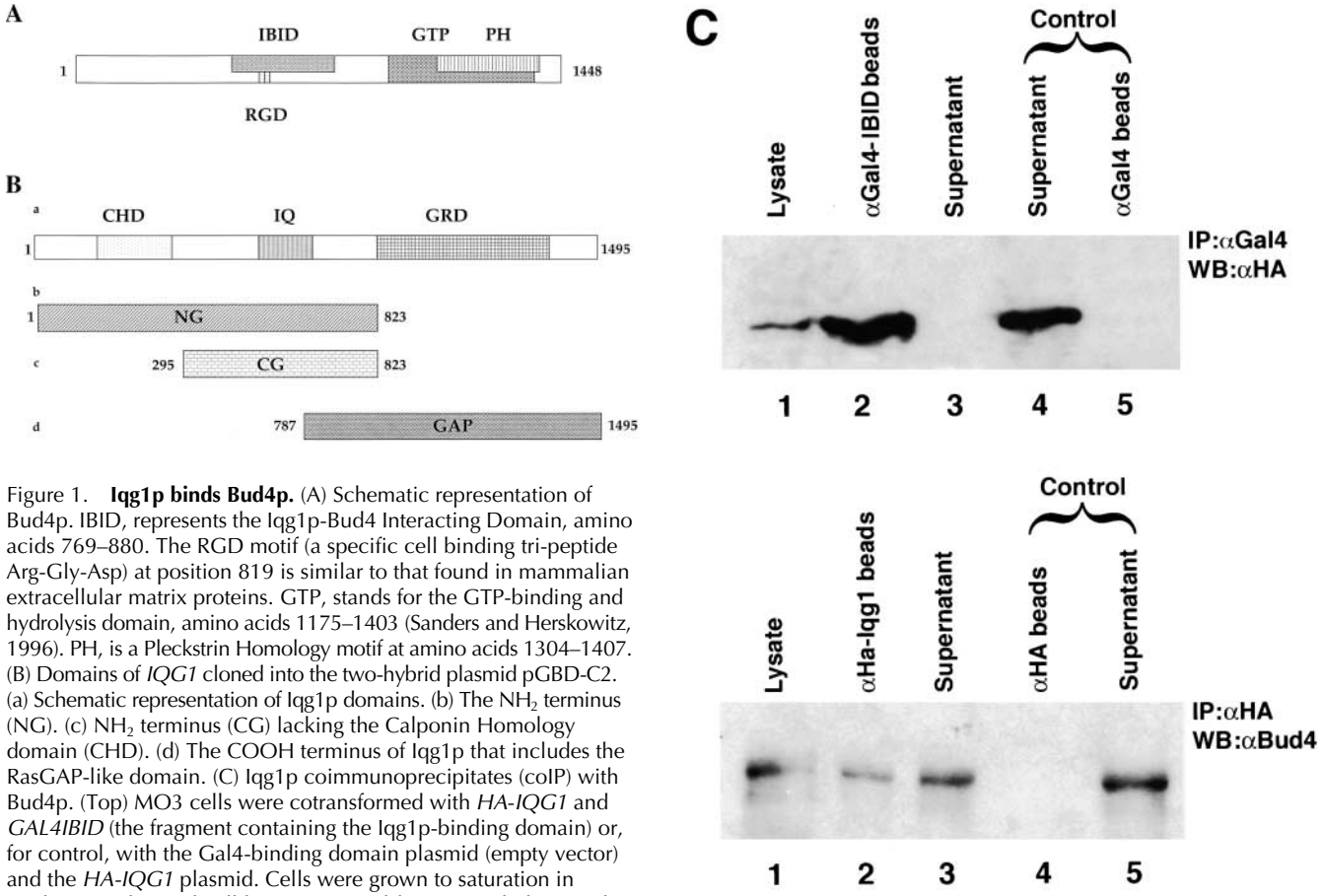

Figure 1. **Iqg1p binds Bud4p.** (A) Schematic representation of Bud4p. IBID, represents the Iqg1p-Bud4 Interacting Domain, amino acids 769–880. The RGD motif (a specific cell binding tri-peptide Arg-Gly-Asp) at position 819 is similar to that found in mammalian extracellular matrix proteins. GTP, stands for the GTP-binding and hydrolysis domain, amino acids 1175–1403 (Sanders and Herskowitz, 1996). PH, is a Pleckstrin Homology motif at amino acids 1304–1407. (B) Domains of *IQG1* cloned into the two-hybrid plasmid pGBD-C2. (a) Schematic representation of Iqg1p domains. (b) The NH_2 terminus (NG). (c) NH_2 terminus (CG) lacking the Calponin Homology domain (CHD). (d) The COOH terminus of Iqg1p that includes the RasGAP-like domain. (C) Iqg1p coimmunoprecipitates (coIP) with Bud4p. (Top) MO3 cells were cotransformed with *HA-IQG1* and *GAL4IBID* (the fragment containing the Iqg1p-binding domain) or, for control, with the Gal4-binding domain plasmid (empty vector) and the *HA-IQG1* plasmid. Cells were grown to saturation in cm-leu-trp. The total cell lysate was used for coIP with the α-Gal4 binding domain antibody. Western blot analysis was performed using an α-HA antibody to detect HA-tagged Iqg1p. (Bottom) MO3 cells were transformed with *HA-IQG1* plasmid or with empty vector as a control. Total cell lysate was used for coIP with α-HA antibodies and Western blot analysis was performed using affinity-purified α-Bud4p antibodies.

possibility for the Cdc42 effector is a member of the family of IQGAPs.

We and others isolated the mammalian IQGAPs-1 and -2 as putative target/effectors for Cdc42p (Hart et al., 1996; McCallum et al., 1996; Erickson et al., 1997). The mammalian IQGAPs were localized to cell–cell junctions (Hart et al., 1996; Kuroda et al., 1996; Bashour et al., 1997), as well as to Golgi membranes (McCallum et al., 1998), with the latter finding suggesting their possible involvement in protein trafficking events. To better understand the cellular functions of the IQGAP family of proteins, we isolated and characterized the yeast homologue, Iqg1p, and found that the *IQG1*-null strain produced phenotypes consistent with the involvement of Iqg1p in both polarity and cytokinesis (Osman and Cerione, 1998). Other groups have shown Iqg1 (Cyk1p) to be essential (Epp and Chant, 1997; Lippincott and Li, 1998) and to participate in an actomyosin-based contractile ring function. However, because the actomyosin ring was found to be dispensable for both cytokinesis and yeast cell growth (Bi et al., 1998), Iqg1p must play additional roles in the cell. Here we report that Iqg1p determines the axial budding pattern, interacts with and promotes the localization of the axial markers Bud4p and Cdc12p, and functionally interacts with the secretion marker, Sec3p. Overall, these findings raise the interesting possibility that the Cdc42p target, Iqg1p, serves to interface proteins involved in a key polarity-dependent process (axial budding) with proteins involved in exocytosis/secretion and cytokinesis.

Results

Identification of Bud4p as an Iqg1p binding partner

To investigate the role of Iqg1p in polarity and cytokinesis, we used the full-length *IQG1*gene in a two-hybrid system (James et al., 1996) to isolate candidate binding partners. In this study, we focus on one clone we identified as *BUD4*. The region of Bud4p that spans amino acids 769–880 ap-

Table I. **Interaction of Bud4p with different domains of Iqg1p**

Iqg1p domain fusion	pGADC 2-BUD4	PGAD-C2
	Miller units	
PGBDC2-Iqg1p (1–1495)	558.67 ± 0.3	0.2 ± 0.3
PGBDC2-Iqg1p (1–823)	502.93 ± 0.5	0.14 ± 0.5
PGBDC2-Iqg1p (295–823)	401.16 ± 0.4	0.2 ± 0.3
PGBDC2-Iqg1p (787–1495)	25.1 ± 0.4	0.2 ± 0.3
pGBDC2	0.22 ± 0.2	0.1 ± 0.3

β-Galactosidase activity (Miller units) was calculated from five independent transformants. The unrelated protein lamin on a binding domain plasmid was used as a negative control and shows no binding.

pears to be the interacting domain for Iqg1p (Iqg1-Bud4 interacting domain [IBID];* Fig. 1 A). This region was isolated four times from the two-hybrid library and does not interact with control proteins such as lamin or with the Gal4-binding domain alone. Bud4p was previously identified as an essential protein for axial budding (Chant and Herskowitz, 1991; Chant and Pringle, 1995; Sanders and Herskowitz, 1996). It contains a putative GTP binding motif at its COOH terminus overlapped by a pleckstrin homology domain. At position 819, and overlapped by the IBID, Bud4p has an RGD motif (Fig. 1 A), denoting a specific cell binding tripeptide motif found on adhesive proteins such as fibronectin. Different domains of Iqg1p (Fig. 1 B) were assayed for their ability to interact with Bud4p, and the results indicated that the NH_2-terminal half of Iqg1p (residues 1–823) contains the Bud4-binding site (Table I).

Iqg1p coimmunoprecipitates with Bud4p

To establish whether Iqg1p binds Bud4p in cells, we transformed a high-copy HA-tagged *IQG1* plasmid into the yeast strain (MO3) lacking the chromosomal copy of the *IQG1* gene (see Materials and methods). We also cotransformed the same strain with both the HA-tagged *IQG1* plasmid and the Gal4-binding domain-tagged *BUD4* plasmid (encoding the IBID) that was isolated from the two-hybrid screen described above. As a control, MO3 cells were also transformed with the vector encoding HA alone, or with both the HA-encoding vector and the Gal4-tagged *BUD4* plasmid containing the IBID domain (Fig. 1 A). The total protein extract was used to isolate immune complexes of either HA-tagged Iqg1p or Gal4-IBID using a monoclonal α-HA antibody (BAbCO) or an α-Gal4 antibody (Santa Cruz Biotechnology, Inc.), respectively. Western blot analysis was performed to detect the presence of Bud4p and HA-tagged Iqg1p in the immune complexes. Fig. 1 C (top) shows that HA-tagged Iqg1p was efficiently coimmunoprecipitated with Gal4-IBID (lane 2), whereas Iqg1p was not coimmunoprecipitated with the Gal4 binding domain alone (lane 5). The bottom panel shows that the endogenous Bud4p coimmunoprecipitated with full-length HA-tagged Iqg1p (lane 2) but not with HA alone (lane 4). As additional controls, we also used other antibodies, such as α-Intersectin and α-GFP, and found that these were unable to coimmunoprecipitate either HA-Iqg1 or Bud4p (unpublished data).

Iqg1p is required for axial budding

To assess whether Iqg1p, like Bud4p, influences the budding pattern, we compared the pattern of the bud scars on the surfaces of haploid and homozygous diploid cells lacking the *IQG1* gene with their isogenic wild-type counterparts. Chitin rings were visualized using Calcofluor as described in the Material and methods. Interestingly, the majority of the haploid cells lacking Iqg1p (∼60%, $n = 400$) exhibited a bipolar budding pattern (Fig. 2 A, A–F) similar to cells lacking *BUD4* (Fig. 2 A, top right). This budding pattern was not observed in the isogenic wild-type cells which showed axial budding (Fig. 2 A, top left), but it appears similar to patterns observed in cells defective in *BUD3* or *BUD4* (Chant and Herskowitz, 1991). Approximately 30% of the *iqg1Δ* cells exhibited a semirandom pattern of budding such that the scars were clustered but not located at the opposite poles (Fig. 2 A, C and D). Another subset of these cells (Fig. 2 A, E and F) showed a distribution of bud scars to the opposite poles but these scars were scattered at the pole and not lined up as in the wild-type cells. Homozygous diploid strains lacking *IQG1* showed the expected bipolar pattern of diploid budding (unpublished data).

Bud4p requires Iqg1p for localization

To determine whether Iqg1p is required for the proper localization of Bud4p to growth sites, we used an affinity-purified Bud4p antibody, a gift from Dr. S. Sanders (Massachusetts Institute of Technology, Boston, MA) (Sanders and Herskowitz, 1996) to compare the localization of Bud4p in wild-type and *iqg1Δ* cells. As expected, in 75% of wild-type cells ($n = 400$) Bud4p localized in two rings at the mother–

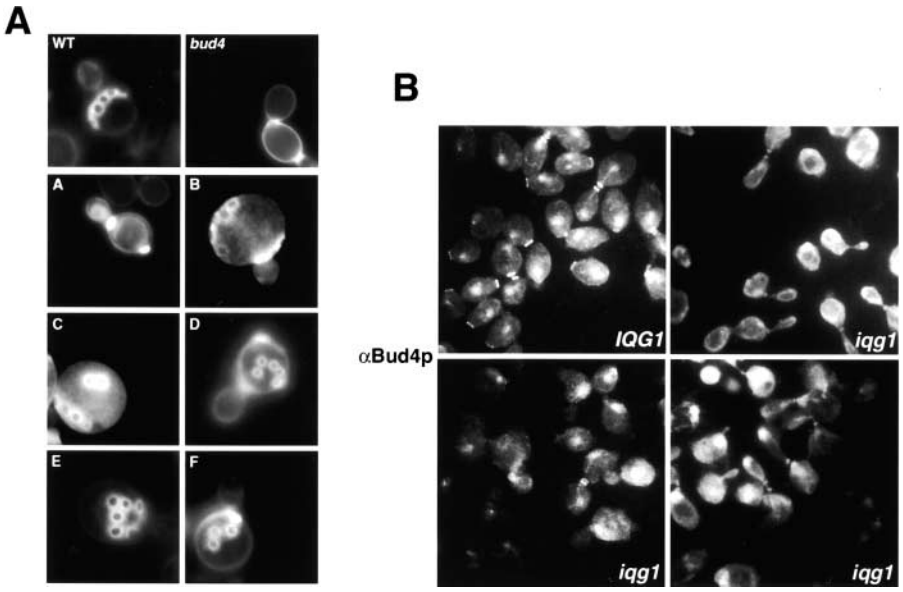

Figure 2. **Iqg1p specifies axial budding and localizes Bud4p.** (A) Iqg1p selects the axial bud-site: wild-type, *bud4Δ*, and *iqg1Δ* cells were grown in YEPD at 26°C, incubated with Calcofluor as described in Materials and methods, and photographed under identical conditions. (A–H) MO3 (*iqg1Δ*) cells. (B) Subcellular localization of Bud4p in wild-type and *iqg1Δ* cells: The subcellular localization of Bud4p was examined in wild-type *IQG1* cells (MO5) and in *iqg1Δ* cells (MO3) as indicated in the panels. Cultures were grown at 23°C overnight, shifted to 30°C for 2 h, fixed with 3.7% formaldehyde and processed for indirect immunofluorescence using an affinity purified anti-Bud4p antibody as described in the Materials and methods.

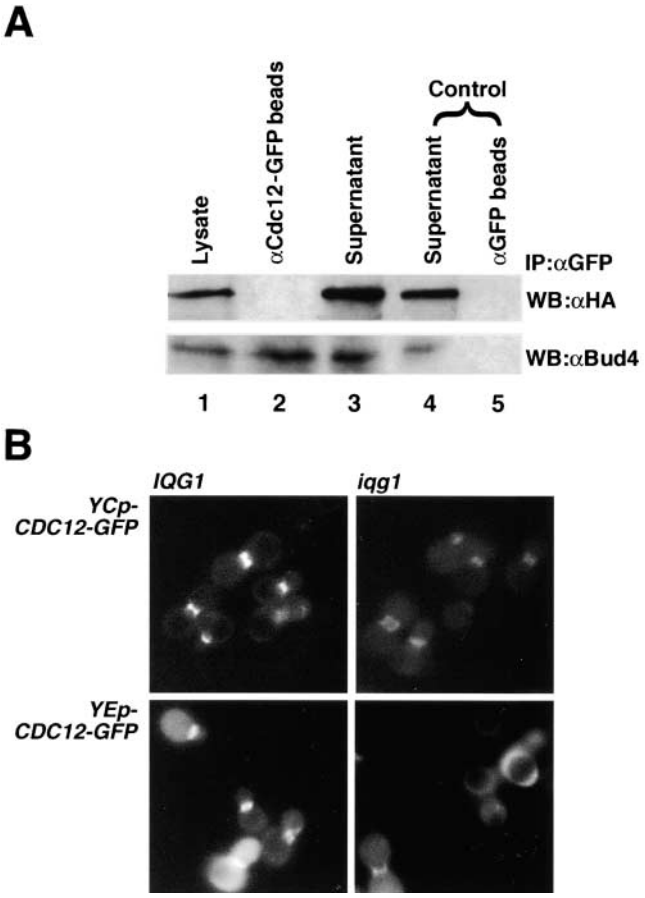

Figure 3. **Interactions between Iqg1p, Bud4p, and Cdc12p.** (A) Examination of the interactions between Cdc12p and either Iqg1p or Bud4p by coimmunoprecipitation. MO3 cells were transformed with *CDC12-GFP* on a low-copy vector and *HA-IQG1* plasmids. Cells were grown to saturation in media lacking uracil and leucine or with GFP empty vector along with the *HA-IQG1* plasmid. The α-GFP antibodies were used to coIP Cdc12p-GFP from total cell lysates. Western blot analysis was performed using α-HA antibodies (top) to detect HA-tagged Iqg1p or affinity-purified α-Bud4p antibodies to detect the endogenous Bud4p (lower panel). The α-Intersectin antibody was used as an additional control. (B) Localization of Cdc12p in wild-type and *iqg1Δ* cells. The subcellular location of a Cdc12p-GFP fusion protein was examined in wild-type *IQG1* cells (MO1) and in *iqg1Δ* cells (MO4) as indicated above the panels. (Top) Cells that carried the *CDC12-GFP* gene on the low-copy vector YCplac111. (Bottom) Cells that carried the *CDC12-GFP* gene on the high-copy vector YEplac181. Cultures were grown overnight at 23°C, shifted to 30°C for 6 h, and then photographed. All photography and printing steps were performed under identical conditions to preserve the different intensities of Cdc12p-GFP fluorescence.

daughter junction and as a ring in unbudded cells (Fig. 2 B, top left; Sanders and Herskowitz, 1996). In 65% of the *iqg1Δ* cells ($n = 400$), Bud4p localization at the neck was either totally abolished or significantly diminished (Fig. 2 B, iqg1-labeled panels). In ~4% of the cells, we detected only one faint ring in the mother cell but not in the daughter cell. In a few cases, we observed a diffuse pattern throughout the cell. However, in no case did we observe a wild-type double ring. These results suggest that Iqg1p is needed to recruit Bud4p to the growth sites.

Table II. **Interaction of Cdc12p with different domains of Iqg1p**

Iqg1p domain fusion	pGADC 2-CDC12	pGAD-C2
	Miller units	
pGBDC2-Iqg1p (1–1495)	23.01 ± 0.3	0.15 ± 0.3
pBDC2-Iqg1p (1–823)	5.79 ± 0.41	0.14 ± 0.32
pGBDC2-Iqg1p (295–823)	4.491 ± 0.2	0.2 ± 0.2
pGBDC2-Iqg1p (787–1495)	18.67 ± 0.15	0.2 ± 0.2
pGBDC2	0.17 ± 0.2	0.1 ± 0.10

β-Galactosidase activity (Miller units) was calculated from six independent transformants.

Efficient septin localization requires Iqg1p

Bud4p was shown to genetically interact with and require the septin, Cdc12p, for localization (Sanders and Herskowitz, 1996). This prompted us to consider the relationship between Iqg1p and Cdc12p. We first used two-hybrid assays to examine the ability of Iqg1p and Cdc12p to interact. These data showed that Cdc12p interacted with the COOH-terminal region of Iqg1p that contains the RasGAP-like domain (Table II). However, thus far, we have not been able to detect the coimmunoprecipitation of a GFP-tagged Cdc12p on a low-copy plasmid with the HA-tagged Iqg1p on a high-copy plasmid (Fig. 3 A, top, lane 2), suggesting that Iqg1p and Cdc12p may undergo a relatively weak or transient interaction. We detected a band for the endogenous Bud4p after immunoprecipitation of Cdc12p-GFP (Fig. 3 A, bottom, lane 2, compare with lane 5), suggesting that these two proteins are able to interact in cells and may bridge the interaction of Iqg1p with Cdc12p.

To further explore the significance of the septin-Iqg1p interaction suggested from the two-hybrid experiments, we examined the localization of Cdc12p in *iqg1Δ* cells, using a Cdc12-GFP construct encoded by either a low-copy (Fig. 3 B, top) or a high-copy vector (Fig. 3 B, bottom). Overall, there was a significant decrease in the intensity of the septin ring in *iqg1Δ* cells (Fig. 3 B, bottoms) compared with wild-type cells (left). The septin ring was completely absent from some *iqg1Δ* cells (bottom right). At 23°C, the permissive temperature for *iqg1Δ* cells, we detected a faint septin ring in 69% of these cells ($n = 102$), whereas a brighter septin ring was observed in 87% of the isogenic wild-type cells ($n = 112$; unpublished data). At 30°C, the semipermissive temperature for *iqg1Δ* cells, we detected a faint septin ring in only 27% of the cells ($n = 365$) compared with 85% of the wild-type cells ($n = 129$). In contrast, the localization of Cdc12p was not affected in *bud4Δ* cells (unpublished data) indicating that only Iqg1p (and not Bud4p) affects Cdc12p localization.

Iqg1p binds and helps localize Sec3p

Sec3p is involved in both bud-site selection and cytokinesis (Haarer et al., 1996; Finger and Novick, 1997). Our previous work implicating Iqg1p in cytokinesis and protein trafficking (Osman and Cerione, 1998), together with the results from this study suggesting that Iqg1p is involved in bud site selection, led us to examine whether there is a functional interaction between Iqg1p and Sec3p. To determine whether Iqg1p associates with Sec3p, we cotransformed the MO3 strain lacking Iqg1p with the high-copy plasmid encoding

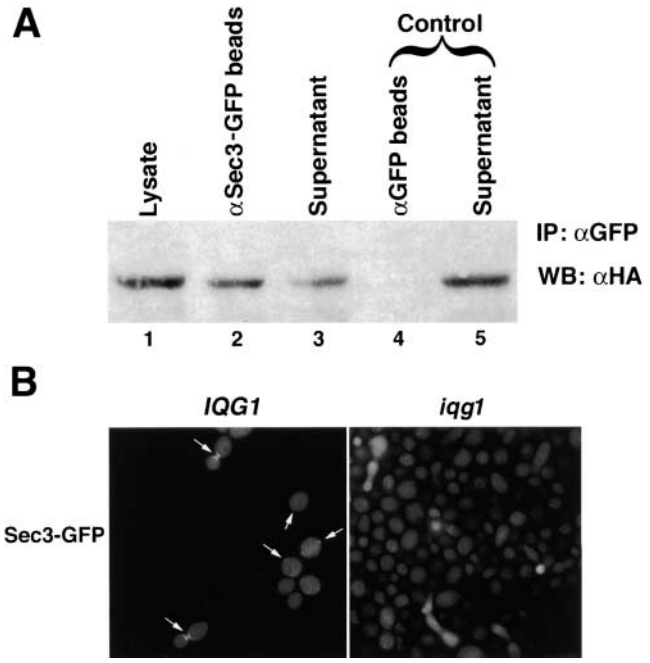

Figure 4. **Iqg1p binds and helps localize Sec3p.** (A) Iqg1p binds Sec3p. MO3 cells were cotransformed with *HA-IQG1* and *SEC3-GFP* plasmids, or with *HA-IQG1* and *GFP* empty vector, and grown to saturation. The total cell lysate was used to immunoprecipitate Sec3p-GFP using α-GFP antibodies along with other control antibodies (α-Intersectin and α-HA). The proteins were fractionated on a 7% SDS-PAGE and the immunoblot was stained with α-HA antibodies to detect HA-Iqg1p. (B) Localization of Sec3p in wild-type and *iqg1Δ* cells. Cells of MOB2 (wild-type; left) and MOB4 (*iqg1Δ*; right), were transformed with the *SEC3-GFP* on a low-copy vector, grown in cm-uracil at 26°C and treated as described in the Materials and methods, visualized and photographed under identical conditions.

HA-tagged Iqg1p (which complements the *iqg1Δ* phenotype), together with either a *SEC3-GFP* on low-copy plasmid (Finger et al., 1998) that complements the *sec3Δ* strains, or the GFP plasmid. Coimmunoprecipitation experiments showed that HA-Iqg1p associated with Sec3p-GFP (Fig. 4 A, lane 2) but not with GFP alone (lane 4), nor was HA-Iqg1p immunoprecipitated with other control antibodies (e.g., α-Intersectin or α-Gal4 antibodies; unpublished data).

To examine the localization of Sec3p in the *iqg1Δ* strain, we transformed the *SEC3-GFP* construct (Finger et al., 1998) into the haploid segregants resulting from one of the tetratype tetrads obtained from the cross between *sec3Δ* and *iqg1Δ* (see below and Table III). In 65% of the wild-type cells (n = 400 cells), Sec3p-GFP localized to the cell poles and as two rings at the mother–daughter neck (Fig. 4 B, left, arrows), as previously reported (Finger et al., 1998). In ~65% of the wild-type cells that appeared to be in G1we also observed two or more cortical Sec3-GFP loci and often a punctate pattern (Fig. 4 B; unpublished data). However, in *iqg1Δ*cells (>400 cells examined), Sec3p-GFP localization at growth sites was abolished and was diffusely distributed throughout the cell (Fig. 4 B, right). Thus, these results suggest that Iqg1p is required for the localization of Sec3p to the sites of polarized growth.

Sec3p and Iqg1p cooperate in axial budding

To begin to investigate the cellular function of the Iqg1p-Sec3p interaction, we crossed BHY51, which harbors the temperature-sensitive *sec3Δ* (Haarer et al., 1996), with the temperature-sensitive *iqg1Δ* (MO3) strain. The resultant diploid was sporulated and twenty-one tetrads were dissected. Each produced four live spores at room temperature. When scored for temperature sensitivity, we obtained 4 PD: 4 NPD: 12 TT tetrads. The tetratype tetrads that produced three temperature-sensitive spores at 37°C were analyzed by PCR to identify the progenies (MOB1–4) for subsequent comparative studies (Table III). In every case examined, one of the temperature-sensitive spores contained the double deletion. The growth and the phenotypes of the segregants from the same tetrad were examined. Compared to wild-type cells (Fig. 5, top left), *sec3Δ* cells showed normal budding and they were temperature-sensitive at 37°C (Fig. 5, middle left). The *iqg1Δ* cells displayed elongated buds (Fig. 5, bottom) and they were temperature-sensitive at 37°C as we previously reported (Osman and Cerione, 1998). In contrast, the double mutant cells exhibited a lower nonpermissive temperature (30°C). At room temperature, the *iqg1Δ sec3Δ* double mutant cells displayed a mixture of budding phenotypes, all consistent with polarity defects (Fig. 5, a–e). These double mutant cells were generally large with wide necks. Some cells showed a bottle-like shape with

Table III. **Yeast strains used**

Strain	Genotype	Source
MO2	*MATa* Gal+ *ura3-52leu2-3, 112 his3 Δ200 lys2-801 iqg1:: HIS3*	Osman and Cerione, 1998
MO3	*MATα* Gal+ *ura3-52leu2-3, 112 his3 Δ200 lys2-801 iqg1:: HIS3*	Osman and Cerione, 1998
SY298	*MATα ura3-52, his4 trp1 MAL2 bud4 :: TRP1*	Sylvia Sanders
BHY51	*MATa ura3 leu2 lys2 his3 trp1 sec3 Δ :: LEU2*	Brian Harrer
MOB1	*MATa* of (BHY51 X MO3), *ura3-52leu2-3, 112 his3 Δ200 lys2sec3 Δ :: LEU2*	This study
MOB2	*MATα* of (BHY51 X MO3), *ura3-52leu2-3, 112 his3 Δ200 lys2*	This study
MOB3	*MATa* of (BHY51 X MO3) *ura3-52leu2-3, 112 his3 Δ200 lys2 sec3 Δ :: LEU2 iqg1 :: HIS3*	This study
MOB4	*MATα* of (BHY51 X MO3), *ura3-52leu2-3, 112 his3 Δ200 lys2 iqg1:: HIS3*	This study
MO1A	*MATα* progeny of BHY51 X SY298 *bud4 :: TRP1*	This study
MO1B	*MATa* progeny of BHY51 X SY298 WT	This study
MO1C	*MATa* progeny of BHY51 X SY298 *sec3 Δ :: LEU2*	This study
MO1D	*MATα* progeny of BHY51 X SY298 *bud4 :: TRP1 sec3 Δ :: LEU2*	This study
PJ69-4A	*MATa trp1-901 leu2,3-112 ura3-52 his3-200 gal4 Δ gal180Δ GAL2-ADE2 LYS::GAL1-HIS3 met2::GAL7-lacZ*	James et al., 1996

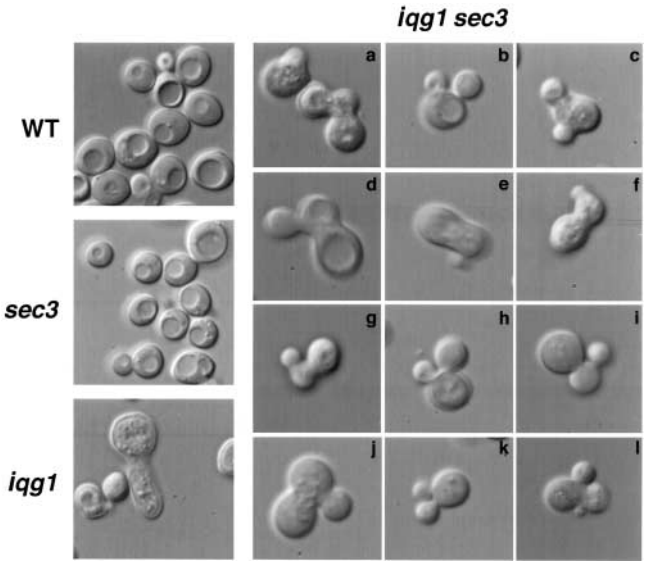

Figure 5. **Polarity defects of *sec3Δ iqg1Δ* cells.** Wild-type, *sec3Δ*, *iqg1Δ* (left) as well as MOB3 (*iqg1Δsec3Δ*) (right, a–l) are shown. Cells were grown in YEPD at 26°C and directly visualized by Nomarski optics and photographed under identical conditions.

an elongated mother containing a wide constriction in the middle, often with a small bud at one side or at one end (e and f). Other cells had two buds, where in many cases both buds originated from the mother cell (b, c, and h), and in some cases, a new bud extended from the older bud (d, g, and i).

Because failure of targeted secretion results in more generalized chitin deposition, we used Calcofluor to analyze the secretion of cell wall material in these mutants. Fig. 6 A shows that in the double mutant cells, chitin is uniformly localized in the mother cell wall, but was not directed to the small bud (6 A, bottom right, arrows). This was not the case in *iqg1Δ* single mutants where chitin was uniformly distributed in both the mother cells and the buds (Osman and Cerione, 1998; unpublished data). In *sec3Δ* cells, we have consistently observed that chitin is only slightly diffuse (Fig. 6 A, top right) but correctly directed to the buds and the bud scars (Haarer et al., 1996; unpublished data).

We also used Calcofluor to measure the budding pattern on the cell surfaces of the haploid progenies described above. Surprisingly, unlike each of the single mutants (Fig. 2 A; unpublished data), the haploid double mutant *iqg1Δ sec3Δ* cells all exhibited random budding patterns (Fig. 6 B, A–E) reminiscent of *BUD1* or *BUD2* defective cells (Chant and Herskowitz, 1991). Only homozygous diploid strains of *sec3Δ* were previously shown to exhibit a random budding (Haarer et al., 1996; Finger and Novick, 1997). However, the results presented in Fig. 6 B suggest that Sec3p affects the budding of haploid cells as well.

Sec3p and Bud4p cooperate for cytokinesis

Because Iqg1p binds and helps localize both Sec3p and Bud4p, we further examined the relationship between Bud4p and Sec3p in a number of different ways. First, we took a genetic approach and crossed BHY51 (*sec3Δ*) with SY298 (*bud4Δ*). The resultant diploid was sporulated and tetrads yielded four live progenies analyzed by PCR to determine their genotypes. The segregants of a single tetratype tetrad (MO1A–D; Table III) were used for further analyses. Some (~10%) of the *bud4Δ* single mutant segregants from this cross revealed a phenotype consistent with a cytokinesis defect (Fig. 7 A, top right). Interestingly, ~30% of the double mutant *bud4Δ sec3Δ* cells displayed chains of 3–5 or more elongated cells (Fig. 7 A, bottom right) that were often branched and remained together after sonication, vigorous vortexing or zymolyase treatment. Another 35% of the double mutant cells displayed shorter chains or appeared as two cells which failed to separate. Moreover, at 30°C, the double mutant cells showed substantial lysis, which was not the case for the single mutants.

Second, we examined the localization of Sec3p in *bud4Δ* cells. The localization of Sec3p-GFP in wild-type cells (Fig. 7 B, middle, inset) was detected in 60% of the total population examined (n = 200); however, its localization was dif-

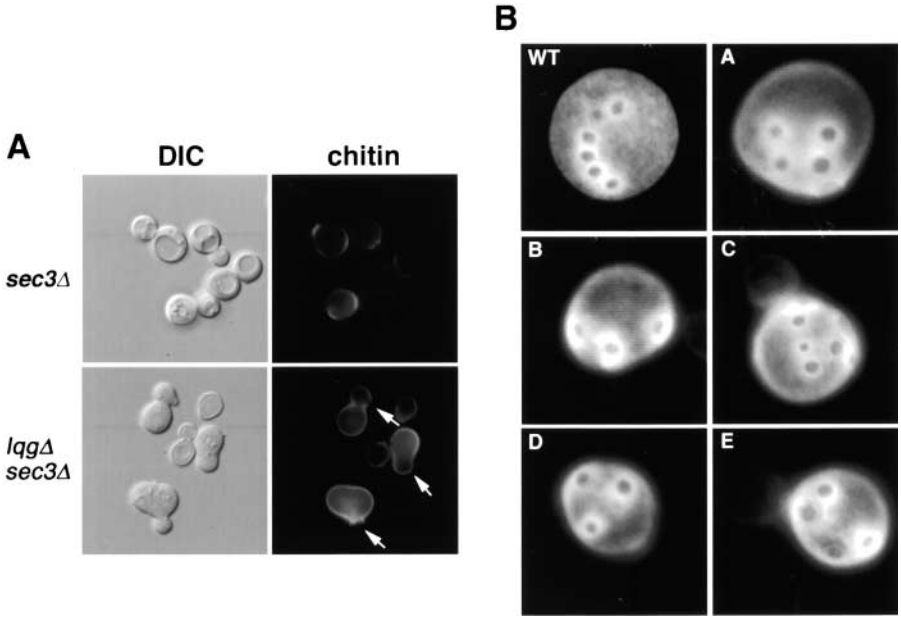

Figure 6. **The *sec3Δ iqg1Δ* cells misdirect chitin to the mother cells and display random budding.** (A) Chitin mislocalization in *sec3Δ iqg1Δ* cells. MOB1 (*sec3Δ*; top), and MOB3 (*sec3Δ iqg1Δ*; lbottom), were grown in YEPD at 26°C and incubated with Calcofluor as described in Materials and methods and photographed. Arrows indicate the smaller buds. (B) Haploid *sec3Δ iqg1Δ* (MOB3) cells display random budding patterns. Cells, grown and treated as above with Calcofluor, were visualized for bud scars (A–E).

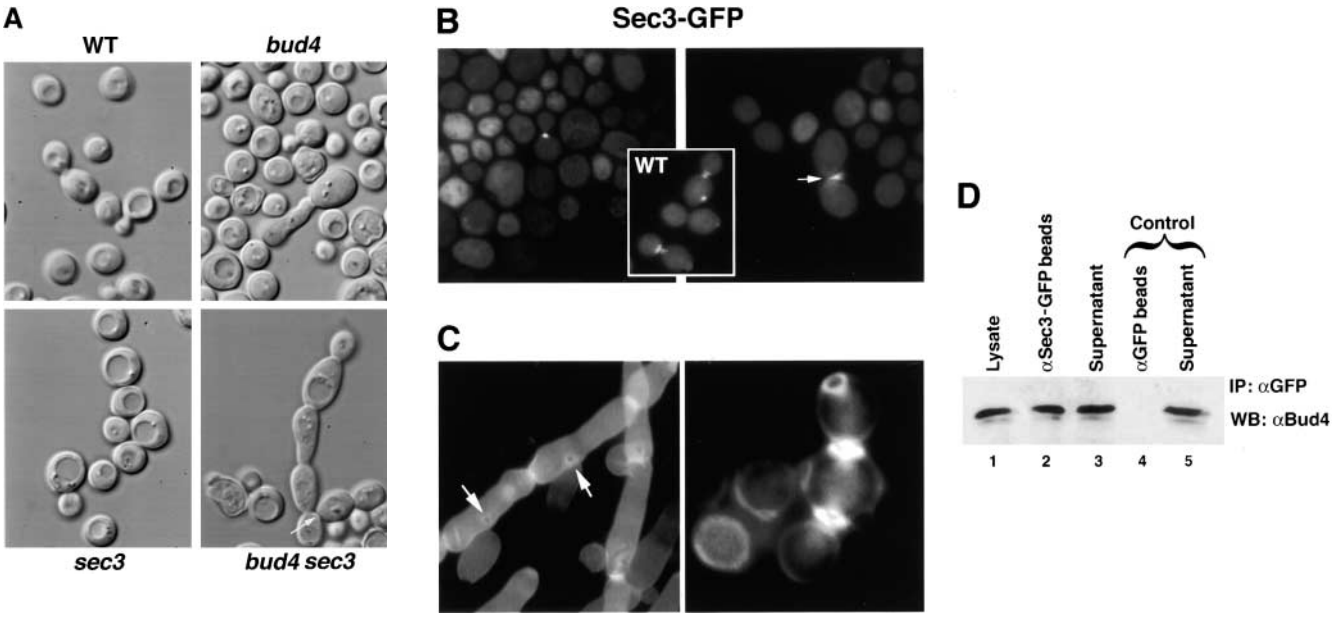

Figure 7. **Bud4p cooperates with Sec3p in cytokinesis.** (A) Phenotype of *bud4Δ sec3Δ* cells. SY298 (*bud4Δ*) was crossed with BHY51 (*sec3Δ)* and the progenies (MO1A-D) of a single tetratype tetrad are shown (Table III). Cells were grown in YEPD at 26°C and directly visualized with Nomarski optics and photographed under identical conditions. (B) Localization of Sec3p in the *bud4Δ* strain. MO1A (*bud4Δ*) and their wild-type counterpart cells (center, inset) were transformed with the *SEC3-GFP* plasmid, grown in cm-uracil at 26°C and treated as in the Materials and methods, and then visualized and photographed under identical conditions. (Left) Diffuse staining of Sec3p-GFP that is typical for *bud4Δ* cells. (Right) Example of the distorted localization of Sec3p-GFP that is observed in a small percentage of the *bud4Δ* cells. (C) Budding pattern of *sec3Δ bud4Δ* double mutants. MO1D (*bud4Δ sec3Δ*) and their wild-type counterparts (not depicted) were grown in YPD at room temperature and stained with Calcofluor (Fluorescent Brightener) and assayed for bud scars. (Left) Elongated chains of cells with the arrows pointing to the branch scars. (Right) Chains of cells displaying bipolar budding only. (D) Bud4p coimmunoprecipitates with Sec3p. MO3 cells transformed with the *SEC3-GFP* on a low-copy vector, or with the *GFP* empty vector, were grown to saturation in cm-uracil and the cell lysate was used to IP Sec3p-GFP with α-GFP antibodies and with other control antibodies (α-Intersectin and α-HA). The proteins were fractionated on a 7% SDS-PAGE and the immunoblot stained with α-Bud4p antibodies.

fuse in *bud4Δ* cells (Fig. 7 B, left). The localization of Sec3p at the incipient bud was undetectable. In only 3% of the cells ($n = 200$) were we able to detect localization of Sec3p-GFP at the mother–bud junction; however, even in these cases, the localization of Sec3p was either extremely faint or distorted in such a way that we did not observe a double ring (Fig. 7 B, right, arrow).

To examine whether Bud4p and Sec3p also cooperate in determining the axial budding pattern, we measured the pattern of bud scars on the cell surface of the *bud4Δ sec3Δ* haploid strain. Approximately 70% of the double mutants displayed bipolar budding pattern (Fig. 7 C, right, chain of cells), similar to that of *bud4Δ* single mutants. However, in ∼60% of those cells, we observed a branching scar that appeared on the surface of the double mutant cells (Fig. 7 C, left, arrows). This scar appears to be the point of a branch of a shorter chain of cells (Fig. 7 A, bottom right, arrow).

Finally, we investigated whether Sec3p-GFP on a low-copy plasmid (Finger et al., 1998) coimmunoprecipitates with endogenous Bud4p. Fig. 7 D shows that a Bud4p band was detected in the immune complexes with Sec3p-GFP (lane 2) but was not detected when immunoprecipitation was performed with control antibodies or with GFP alone (Fig. 7 D, lane 4).

Table IV. **Interaction of Mlc1p and Cmd1p with different domains of Iqg1p and with Bud4**

Iqg1p domain fusion	pGADC2-MLC1	pGADC2-CMD1	pGADC2
		Miller units	
pGBDC2-Iqg1p (1–1495)	98.67 ± 0.6	50.08 ± 0.2	0.2 ± 0.3
pGBDC2-Iqg1p (1–823)	106.91 ± 0.7	107.2 ± 0.1	0.14 ± 0.5
pGBDC2-Iqg1p (295–823)	408.21 ± 0.4	36.67 ± 0.5	0.2 ± 0.3
pGBDC2-Iqg1p (787–1495)	20.1 ± 0.4	18.00 ± 0.2	0.2 ± 0.3
pGBDC2	0.23 ± 0.2	0.25 ± 0.2	0.2 ± 0.3
Construct			
pGBDC2-MLC1/ pGAD-BUD4		66.083 ± 0.5	
pGBDC2-MLC1/pGADC2		0.23 ± 0.2	

β-Galactosidase activity (Miller units) was calculated from four independent transformants of each.

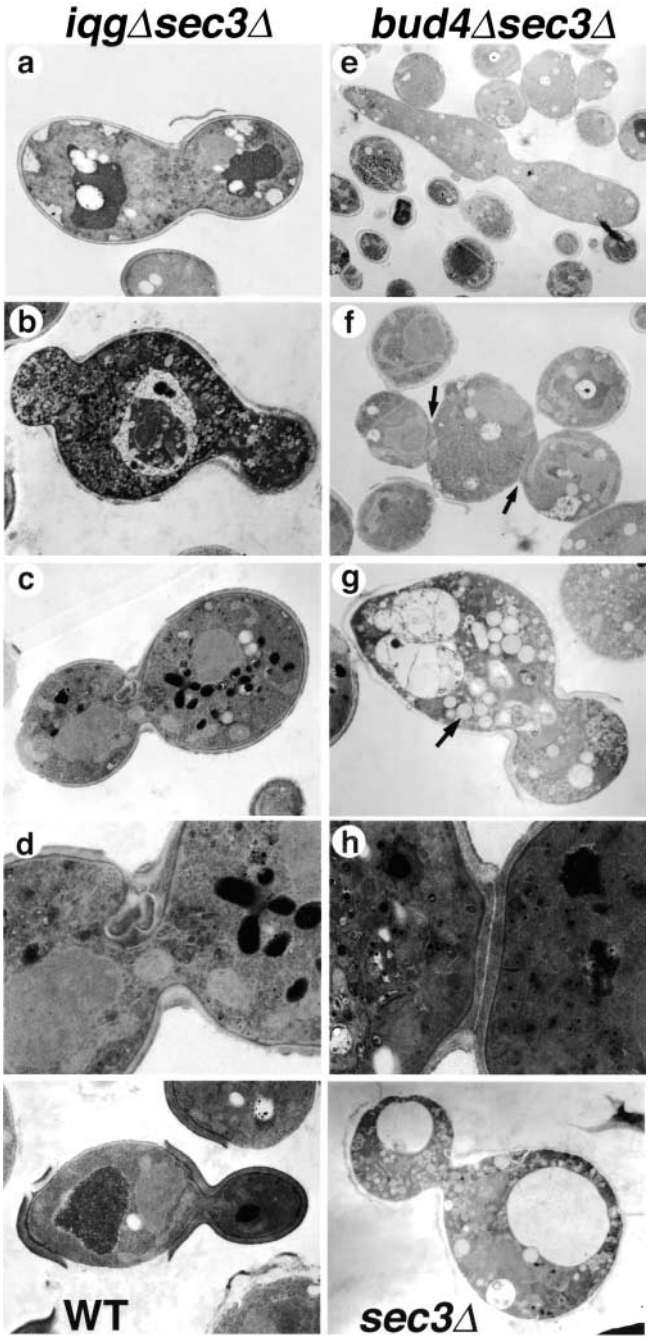

Figure 8. **Septal defects of *iqg1Δ sec3Δ* (MOB3) and *bud4Δ sec3Δ* (MO1D) cells.** Cells were grown to log phase at 25°C and shifted to 37°C for 30 min and then fixed at room temperature and processed for thin section as described in the Materials and methods. (a–d) Examples of *iqgΔ sec3Δ* cells. (e–h) Examples of *bud4Δ sec3Δ* cells. (f and g, arrows) Vesicles and the septa at the necks of the *bud4Δ sec3Δ* cells. Panels d and h are enlargements of the neck region. (Bottom, left and right) Wild-type and *sec3Δ* cells, respectively.

Septal deposition defects are observed in the double mutants

To study the subcellular effects of the double deletion of *IQG1* and either *BUD4* or *SEC3*, we examined the cells by thin-section electron microscopy after shifting to the nonpermissive temperature (37°C) for 30 min. As reported previously (Finger and Novick, 1997), *Sec3Δ* cells accumulated vesicles all over the mother cell and the bud (Fig. 8, bottom right). Interestingly, in both of the double-deletion strains (n = 150 each), these vesicles were either no longer visible or in some cases, fused into larger vesicular structures, especially in *bud4Δ sec3Δ* cells (Fig. 8 g, arrows). In contrast to wild-type and single-mutant cells, the double-mutant cells showed septal defects and in some cases, broad necks. In ~58% of the *iqg1Δsec3Δ* cells (n = 100), the septa were either absent (Fig. 8, a and b) or aberrant (panels c and d). In *bud4Δsec3Δ* cells, the picture was slightly different. We either detected no septa (Fig. 8, e and g) or, in ~3% of the cells, we detected septa that remained intact in a broad neck (Fig. 8, f, arrows, and h), especially within the chains of cells. These defects suggest that Iqg1p, Bud4p, and Sec3p all contribute to proper septum deposition and separation.

Iqg1p connects the myosin light chain, mlc1p, to spatial markers

From the same two-hybrid screen described earlier, we also isolated the Myosin light chain protein, Mlc1p, using full-length Iqg1p as bait. Table IV shows the mapping of the interaction of Iqg1p with Mlc1p, compared to its interaction with Calmodulin, Cmd1p. Mlc1p interacts with the region harboring the IQ motifs of Iqg1p, whereas Cmd1p interacts with a region within the NH_2-terminal half of Iqg1p distinct from the IQ motif. These in vivo results are consistent with the in vitro results reported by Shannon and Li (1999, 2000). In addition, we detected a two-hybrid interaction between Mlc1p and Bud4p, although thus far, we have been unable to detect this interaction in coimmunoprecipitation experiments.

Discussion

We have previously shown that Iqg1p influences polarity, cytokinesis and protein trafficking (Osman and Cerione, 1998). Here we present data addressing the mechanism by which Iqg1p influences these processes. We have identified Iqg1p binding partners that function together in axial bud site selection and cytokinesis. Given that Iqg1p serves as a target/effector for Cdc42p (Osman and Cerione, 1998), these results also provide additional molecular evidence for the involvement of Cdc42p in coordinating polarity establishment and bud site selection with cytokinesis.

The axial budding pattern in haploid yeast is spatially programmed by Bud3p, Bud4p, Axl1p, and the transmembrane protein Bud10p (for review see Chant, 1999). Using a two-hybrid screen, we have identified Bud4p as an Iqg1p-binding partner (Table I). We further demonstrated that Iqg1p was co-immunoprecipitated with Bud4p (Fig. 1 C) and was required for its localization (Fig. 2 B). We showed that, like Bud4p, Iqg1p specifies axial budding in yeast. Haploid cells lacking *IQG1* displayed bipolar budding (Fig. 2 A) similar to *bud4Δ* mutants, while the isogenic homozygous diploid cells were unaffected. This axial budding defect (Fig. 2 A) suggests that Iqg1p works together with Bud4p to specify axial bud site selection. However, the fact that Bud4p is localized as a spatial marker in the previous cell cycle, and loses this localization at the neck in *iqg1Δ* cells (Fig. 2 B), supports the idea that Iqg1p recruits Bud4p as an axial marker.

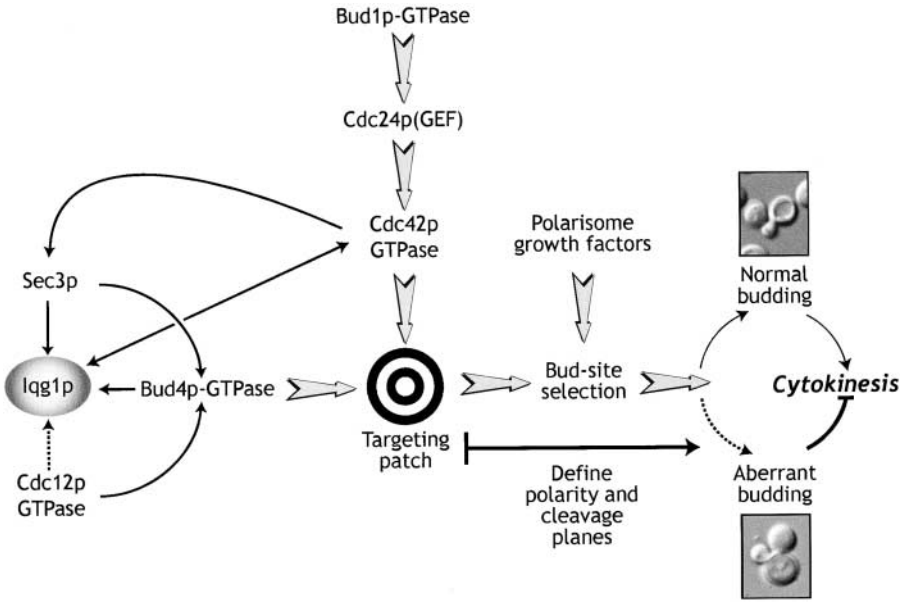

Figure 9. **A model for a mechanism of action of Iqg1p in cytokinesis.** A model depicting the role of Iqg1p in determining polarity and cytokinesis by organizing a polarity (bud-site) targeting patch operating as a checkpoint for cytokinesis. In the absence of an Iqg1p–protein complex, alternative pathways lead to a second round of (aberrant) budding resulting in polarity and cytokinesis defects. By binding and localizing both Cdc42p (double arrow; Osman and Cerione, 1998) and Bud4p, Iqg1p connects the polarity establishment modules to the bud-site selection tags.

Iqg1p also appears to interact with and helps localize the septin Cdc12p (Table II; Fig. 3 B), which is necessary for both cytokinesis and axial budding (for review see Chant, 1996, 1999; Madden and Snyder, 1998). Bud4p may mediate the interaction between Iqg1p and Cdc12p, as we have detected the coimmunoprecipitation of Cdc12p and Bud4p, but have not yet been able to detect an interaction between Cdc12p and Iqg1p in coimmunoprecipitation experiments (Fig. 3 A). However, we have found that Iqg1p, and not Bud4p, affects the efficient localization of the septin Cdc12p to the neck (Fig. 3 B; unpublished data), further supporting the idea that Iqg1p assembles the proteins required for axial budding. In addition, the interaction between Iqg1p, Bud4p, and Cdc12p may involve a cooperation in some aspect of cytokinesis, as both Iqg1p and septins have been previously implicated in this process.

Several lines of evidence presented in this study indicate that Iqg1p and Sec3p work together to influence cell polarity, axial budding and cytokinesis in yeast. We have provided evidence that Iqg1p coimmunoprecipitates with (Fig. 4 A) and is required for the localization of Sec3p (Fig. 4 B). The *iqg1Δsec3Δ* double mutants displayed a lower restrictive temperature and exhibited phenotypes consistent with a polarity defect (Fig. 5) that resulted in random budding (Fig. 6 B). These double mutants also failed to direct growth material to the new bud (Fig. 6 A) and to form correct septa at the mother-daughter junctions (Fig. 8).

Together, these results suggest a role for Sec3p in axial budding. Although earlier studies have suggested that Sec3p is primarily involved in diploid budding (Haarer et al., 1996; Finger and Novick, 1997), our findings are consistent with the idea that targeted secretion is required for budding in both cell types (for review see Finger and Novick, 1998). Our data also suggest that Iqg1p works with Sec3p to maintain cell polarity. Figs. 5 and 6 B show that budding in the *iqg1Δ sec3Δ* double mutant strain was initiated normally but was not maintained such that another bud originated either from the mother, the bud (Fig. 5) and/or at a random location (Fig. 6 B). This may reflect the actions of polarity establishment proteins such as Cdc42p and Bud1p. Iqg1p may mediate the interplay between the bud site selection function of the Bud1 GTPase and the maintenance of polarity by Cdc42p (Fig. 9). Three independent pieces of evidence seem to support this view. First, the random budding phenotype of the *iqg1Δ sec3Δ* double mutant cells (Fig. 6 B) is similar to that of *bud1Δ* or *bud2Δ* mutant cells (Chant and Herskowitz, 1991). Second, analyses of *bud1Δ cdc24Δ* cells revealed that the essential role of the polarity establishment molecules in morphogenesis is to stabilize the axis of polarity, and that in their absence, this axis wanders (Nern and Arkowitz, 2000). Third, a recent study demonstrated direct binding between Sec3p and Cdc42p (Zhang et al., 2001) and showed that Sec3p was mislocalized in cells expressing certain mutations of Cdc42p. Together, these data support the idea that the Cdc42p target Iqg1p coordinates the positional signal for budding and secretion with the signal to maintain polarity and promote cytokinesis.

There also appears to be a functional interplay between Bud4p and Sec3p in budding and cytokinesis. Bud4p can be coimmunoprecipitated with Sec3p (Fig. 7 D) and the proper localization of Sec3p is nearly abolished in the absence of Bud4p (Fig. 7 B). Furthermore, the *bud4Δsec3Δ* double mutants displayed a lower nonpermissive temperature and exhibited budding defects (Fig. 7 C). In addition, the phenotype of *bud4Δsec3Δ* cells highlights a possible role for Bud4p in cytokinesis (Fig. 7 A), apparently, in the final stages of cell separation (Fig. 8). Iqg1, Bud4p and Sec3p may work together to ensure proper septum formation or deposition, thus explaining the wide and aberrant neck formation reported in some *sec3Δ* cells (Finger and Novick, 1997), as well as that observed in *sec3Δ bud4Δ* cells, or the absence of septa in *iqg1Δ sec3Δ* cells (Fig. 8). Overall, our findings appear to be consistent with the "cytokinesis tag" model for axial budding. This model predicts that components involved in cytokinesis are also involved in selecting the future bud-site. The subsequent activation of the Bud1 GTPase then directs the assembly and the initiation of the new bud at that site (for review see Madden and Snyder, 1998).

In conclusion, we propose that Iqg1p forms a targeting patch that includes Bud4p, Cdc12p, and Sec3p (Fig. 9). This protein complex may play a primary role in cytokinesis by first determining, and then maintaining, the axis of polarity by choosing a bud site. The complex would recruit the exocyst for targeted secretion and other morphogenetic factors such as Mlc1p and Cmd1p (Table IV) to promote bud growth and eventually lead to septum deposition and separation. In this way, the Iqg1 complex would in effect serve as a checkpoint for cytokinesis by preventing another round of budding until cytokinesis is complete (Fig. 9). In the absence of the Iqg1p-targeting complex, alternative pathways for budding can apparently bypass the checkpoint leading to rounds of budding and chains of cells observed in the double mutants.

Materials and methods

Isolation of Bud4p as an Iqg1p binding partner

The PCR-amplified *IQG1* gene was cloned in frame into pGBD-C2 to produce the Gal4 binding domain Iqg1p fusion protein. This plasmid was used to screen three yeast genomic libraries, YL2H-C1-3, using the yeast strain PJ694A (James et al., 1996). The interacting library plasmid was subsequently transformed into *Escherichia coli*, purified, and sequenced to identify Iqg1p binding partners. The Iqg1p domain deletions shown on Fig. 1 B were generated by PCR and cloned into *pGBD-C2* to further delineate the binding domain for Bud4p, Cdc12p, Mlc1p, and Cmd1p.

Coimmunoprecipitation experiments

For coimmunoprecipitation experiments, tagged plasmids were cotransformed into a strain lacking the chromosomal copy of *IQG1*. To examine the coimmunoprecipitation of Iqg1p and Bud4p, cells were grown in synthetic complete media (cm) lacking tryptophan and leucine after transformation with HA-tagged Iqg1p on a high copy plasmid (pA1; Osman and Cerione, 1998) and Gal4-IBID (amino acids 769–880 from Bud4p, Fig. 1 A). Cells harboring HA-Iqg1p (pA1) alone were grown in cm-leucine. For control experiments, cells were transformed with parent plasmids lacking the relevant gene. When examining the interaction between Iqg1p and Cdc12, MO3 cells were transformed with *CDC12-GFP* on a low copy plasmid (described below) and *HA-IQG1*, and grown on cm-uracil and leucine. When examining the coimmunoprecipitation of Iqg1p and Sec3p, MO3 cells transformed with *SEC3-GFP* on a low-copy plasmid (Finger et al., 1998) and *HA-IQG1* were grown in cm media lacking uracil and leucine. In all cases, the cell cultures were grown to saturation and the cell pellets washed with and suspended in cold IP-buffer (50 mM Tris, pH 7.5, 1 mM EDTA, 5% glycerol, 0.1% Triton, 1 mM PMSF and fungal protease inhibitor cocktail [Sigma-Aldrich]). Acid-washed glass beads (Sigma-Aldrich) were added to break the cells by vortexing and the cell lysates were collected after centrifugation at 20,000 rpm at 4°C. Two mL of the total cell lysate (scaled up for Sec3p-Iqg1p experiments) was incubated with antibodies (a control antibody was also included) for 3 h with gentle rocking at 4°C. 4 mg of IP buffer-washed protein A Sepharose (Sigma-Aldrich) was added to the immune complexes and incubated overnight at 4°C with gentle rocking. The reaction mix was centrifuged at 10,000 rpm for 30 s and the bead portion was washed four times with ice-cold IP buffer, suspended in 30 μL SDS-loading buffer, boiled at 100°C and separated by 7-10% SDS-PAGE. Western blot analyses were performed using standard methods.

Fluorescence microscopy

To visualize chitin deposition and bud scars on the yeast cell wall, cells were collected at log phase and stained with Calcofluor (Fluorescent Brightener; Sigma-Aldrich) as described (Pringle, 1991). Cells with three or more bud scars were scored for budding pattern. For Cdc12p localization, a *CDC12-GFP* fusion gene was constructed by using PCR to fuse an enhanced version of the GFP (Cormack et al., 1997) to the carboxyl terminus of Cdc12p. The *CDC12-GFP* gene was cloned into the low-copy vector YCplac111 and also into the high-copy vector YEplac181 (Gietz and Sugino, 1988). Wild-type (MO5) and *iqg1Δ* cells (MO2) carrying the indicated *CDC12-GFP* plasmid, or a control vector, were grown overnight at 23°C and then adjusted to 10^6 cells/mL and shifted to 30°C for 6 h. The cells were then examined using an Olympus BH2 fluorescence microscope, photographed with Kodak TMAX400 film, and then the negatives were scanned into digital images under identical conditions. By comparing different exposures, we found that it requires at least a fourfold longer exposure to see similar neck staining in MO2 than in MO5. *CDC12-GFP* fluorescence was better at 23°C in the MO2 strain, but was still weaker than the wild-type strain.

Strains resulting from single tetratype tetrads of the cross between either SY298 (*bud4Δ*) or MO3 (*iqg1Δ*) with *sec3Δ* were transformed with a *SEC3-GFP* plasmid (Finger et al., 1998) which encodes GFP fused to the COOH terminus of Sec3p. Log phase cells growing in cm-uracil liquid media were processed as described in (Finger et al., 1998) and visualized under 100× using a Zeiss fluorescence microscope. Images were collected using Axiovision software under identical conditions.

Thin-section electron microscopy

Log phase overnight cultures of wild-type (MOB2 or MO1B), *sec3Δ* (MOB1), *iqg1Δ* (MOB4), *bud4Δ* (MO1A), *iqgΔsec3Δ* (MOB3), and *bud4Δsec3Δ* (MO1D) strains growing at room temperature were adjusted to 0.3 A_{600}nm units/mL in YEPD and incubated at 37°C for 30 min. Cultures were directly fixed in 0.1 M cacodylate containing 2.5% glutaraldehyde and 2.5% paraformaldehyde for 2 h. Cells were treated with 0.2 mg/mL zymolyase 100T in 0.1 M KPi, pH 7.5. The cell pellets were incubated with ice-cold OsO_4 in 0.1 M cacodylate for 1 h, washed twice with water and incubated for 1 h in 1.5 mL of filtered 2% uranyl acetate at room temperature. A series of ethanol concentrations (50, 70, 90, and 100%) were used to dehydrate the cells followed by acetone treatment. The cells were then incubated for a few hours in 50% acetone/50% SPURR (Electron Microscopy Sciences), changed to 100% SPURR, and incubated overnight at room temperature. After changing to SPURR 2×, cells were baked at 80°C for 24 h. This and the rest of the sectioning and processing were carried out at the Cornell Integrated Microscopy Center (Ithaca, NY).

We thank Drs. Sylvia Sanders for Bud4 strains and antibody, Brian Haarer for strains and plasmids, and Peter Novick for the SEC3-GFP construct. We also thank Drs. Juan Lucas and Sigrid Holmgren for helping with tetrad dissection, Dr. David Holowka for critical reading of the manuscript and helpful comments, and Drs. David Pruyne for helpful discussion, and Jianbin Wang for the α-Intersectin antibody used for controls. Thanks to Cindy Westmiller for expert technical assistance. This work was supported by NIH grant RO1 GM47458. MAO was supported by an NIH Training Grant T32 CA09682.

Submitted: 16 May 2002
Revised: 16 October 2002
Accepted: 21 October 2002

References

Bashour, A.-M., A.T. Fullerton, M.J, Hart, and G.S. Bloom. 1997. IQGAP1, a Rac- and Cdc42-binding protein, directly binds and cross links microfilaments. *J. Cell Biol.* 137:1555–1566.

Bi, E., P. Maddox, D.J. Lew, E.D. Salmon, J.N. McMillan, E. Yeh, and J.R. Pringle. 1998. Involvement of an actomyosin ring in *Saccharomyces cerevisiae. J. Cell Biol.* 142:1301–1312.

Bowser, R., H. Muller, B. Govidan, and P. Novick. 1992. Sec8p and Sec15p are components of a plasma membrane-associated 19.5 S particle that may function downstream of Sec4p to control exocytosis. *J. Cell Biol.* 118:1041–1056.

Chant, J. 1996. Septin scaffolds and cleavage planes in *Saccharomyces. Cell.* 84: 187–190.

Chant, J. 1999. Cell Polarity in yeast. *Annu. Rev. Cell Dev. Biol.* 15:365–391.

Chant, J., and I. Herskowitz. 1991. Genetic control of bud site selection in yeast by a set of gene products that comprise a morphogenetic pathway. *Cell.* 65: 1203–1212.

Chant, J., and J.R. Pringle. 1995. Patterns of bud-site selection in the yeast *Saccharomyces cerevisiae. J. Cell Biol.* 129:751–765.

Cormack, B.P., G. Bertram, M. Egerton, N.A. Gow, S. Falkow, and A.J. Brown. 1997. Yeast-enhanced green fluorescent protein (yEGFP) a reporter of gene expression in Candida albicans. *Microbiology.* 143:303–311.

Epp, A.J., and J. Chant. 1997. An IQGAP-related protein controls actin-ring formation and cytokinesis in yeast. *Curr. Biol.* 7:921–929.

Erickson, J.W., R.A. Cerione, and M.J. Hart. 1997. Identification of an actin cytoskeleton complex that includes IQGAP and the Cdc42 GTPase. *J. Biol. Chem.* 272:24443–24447.

Finger, F., and P. Novick. 1997. Sec3 is involved in secretion and morphogenesis in. *Saccharomyces cerevisiae. Mol. Biol. Cell.* 8:647–662.

Finger, F., and P. Novick. 1998. Spatial regulation of exocyst: lessons from yeast. *J. Cell Biol.* 142:609–612.

Finger, F.P., T.E. Hughes, and P. Novick. 1998. Sec3p Is a spatial landmark for polarized secretion in budding yeast. *Cell.* 92:559–571.

Gietz, R.D., and A. Sugino. 1988. New yeast-*Escherichia coli* shuttle vectors constructed with in vitro mutagenized yeast genes lacking six-base pair restriction sites. *Gene.* 30:527–534.

Guo, W., F. Tamanoi, and P. Novick. 2001. Spatial regulation of the exocyst complex by Rho1 GTPase. *Nat. Cell Biol.* 3:353–360.

Haarer, B.K., A. Corbett, Y. Kweon, A.S. Petzold, P. Silver, and S.S. Brown. 1996. SEC3 Mutations are synthetically lethal with profilin mutations and cause defects in diploid-specific bud selection. *Genetics.* 144:495–510.

Hart, M.J., M.G. Callow, B. Souza, and P. Polakis. 1996. IQGAP1, a calmodulin-binding protein with a RasGAP-related domain, is a potential effector for Cdc42Hs. *EMBO J.* 15:2997–3005.

James, P., J. Halladay, and E.A. Craig. 1996. Genomic libraries and a host strain designed for highly efficient two-hybrid selection in yeast. *Genetics.* 144: 1425–1436.

Johnson, D.I., and J.R. Pringle. 1990. Molecular characterization of CDC42, a *Saccharomyces cerevisiae* gene involved in the development of cell polarity. *J. Cell Biol.* 111:143–152.

Kuroda, S., M. Fukata, K. Kobayashi, M. Nakafuku, N. Nomura, A. Iwamatsu, and K. Kaibuchi. 1996. Identification of IQGAP as a putative target for the small GTPase, Cdc42 and Rac1. *J. Biol. Chem.* 271:23363–23367.

Lew, D.J., and S.I. Reed. 1995. Cell cycle control of morphogenesis in budding yeast. *Curr. Opin. Genet. Dev.* 5:17–23.

Lippincott, J., and R. Li. 1998. Sequential assembly of myosin II, an IQGAP-like protein, and filamentous actin to a ring structure involved in budding yeast cytokinesis. *J. Cell Biol.* 140:355–366.

Madden, K., and M. Snyder. 1998. Cell polarity and morphogenesis in budding yeast. *Annu. Rev. Microbiol.* 52:687–744.

McCallum, S.J., W.J. Wu, and R.A. Cerione. 1996. Identification of a putative effector for Cdc42Hs with high sequence similarity to the RasGAP-related protein IQGAP1 and a Cdc42Hs binding partner IQGAP2. *J. Biol. Chem.* 271:21732–21737.

McCallum, S.J., J.W. Erickson, and R.A. Cerione. 1998. Characterization of the Association of the actin-binding protein IQGAP, and activated Cdc42 with Golgi membrane. *J. Biol. Chem.* 273:22537–22544.

Nern, A., and R.A. Arkowitz. 2000. G Proteins mediate changes in cell shape by stabilizing the axis of polarity. *Mol. Cell.* 5:853–864.

Osman, M., and R.A. Cerione. 1998. Iqg1p, a yeast homologue of the mammalian IQGAPs, mediates Cdc42p effects on the actin cytoskeleton. *J. Cell Biol.* 142:443–455.

Pringle, J.R. 1991. Staining of bud scars and mother cell wall chitin with Calcofluor. *Methods Enzymol.* 194:732–735.

Sanders, S.L., and C. Fields. 1995. Bud-site selection is only skin deep. *Curr. Biol.* 5:1213–1215.

Sanders, S.L., and I. Herskowitz. 1996. The BUD4 protein of yeast, required for axial budding, is localized to the mother/BUD neck in a cell cycle-dependent manner. *J. Cell Biol.* 134:413–427.

Shannon, K.B., and R. Li. 1999. The multiple roles of Cyk1p in the assembly and function of the actomyosin ring in budding yeast. *Mol. Biol. Cell.* 10:283–296.

Shannon, K.B., and R.A. Li. 2000. Myosin light chain mediates the localization of the budding yeast IQGAP-like protein during contractile ring formation. *Curr. Biol.* 10:727–730.

TerBush, D.R., and P. Novick. 1995. Sec6, Sec8, and Sec15 are components of a multisubunit complex which localizes to small bud tips in *Saccharomyces cerevisiae. J. Cell Biol.* 130:299–312.

Zhang, X., E. Bi, P. Novick, L. Du, K.G. Kozminski, J.H. Lipschutz, and W. Guo. 2001. Cdc42 interacts with the exocyst and regulates polarized secretion. *J. Biol. Chem.* 276:46745–46750.